

Disrupting Fluorescence by Mutagenesis in a Green Fluorescent Fatty Acid Binding Protein from a Marine Eel

Sara Rose Krivoshik^{1,2} · Andrew M. Guarnaccia^{1,2} · Daniel B. Fried³ · David F. Gruber^{1,2} · Jean P. Gaffney^{1,2}

© Springer Science+Business Media, LLC, part of Springer Nature 2020

Abstract

Biofluorescence has been found to be an increasingly widespread phenomenon in the ocean. The reclusive Caribbean chlop-sid eel, *Kaupichthys hyoproroides* displays bright green fluorescence in its native marine environment. We have previously shown the fluorescence to be attributed to a fluorescent fatty acid-binding protein, Chlopsid FP, part of a larger family of fluorescent fatty acid-binding proteins, including the homologous UnaG. All require the addition of exogenous bilirubin for fluorescence. Here, we report the generation of a series of point mutants, and deletions that result in the quenching of fluorescence in Chlopsid FP. In addition, we report the binding constants of bilirubin to Chlopsid FP and mutants, measured by fluorescence titration. This study provides key insights into the potential mechanism of fluorescence in this class of fluorescent fatty acid-binding proteins.

Keywords Green fluorescence · Chlopsid FP · Fatty acid-binding proteins · Bilirubin · Eel

1 Introduction

The recent discovery of biofluorescence in cartilaginous and bony fishes across over 180 species, has revealed an abundance of biologically-derived fluorescent diversity in the ocean [1, 2]. Biofluorescence is commonly observed in species in the photic zone [3, 4]. In clear ocean water the light spectrum bandwidth progressively narrows with increasing depth, reaching a wavelength peak of 465 nm and a narrow bandwidth of ~ 20 nm at the maximum depth of penetration [5]. In 2011, a reclusive fluorescent eel (*Kaupichthys hyoproroides*) was fortuitously captured on camera, leading to the identification of several fluorescent eels throughout the Caribbean and South Pacific [6]. *Kaupichthys hyoproroides* exhibits bright green fluorescence when excited with blue light. The protein responsible for fluorescence in *K. hyoproroides* is Chlopsid FP, a member of a larger class of

fluorescent fatty acid binding proteins [6]. The first identified member of fluorescent FABPs was identified in the eel, *Anguilla japonica* and named UnaG [7–10]. Despite the wide geographical distribution of fluorescent eels, studies have shown that the amino acid sequences of these fluorescent proteins are highly conserved [6, 11, 12].

The structure of UnaG was solved and bilirubin was found to be required as an exogenous cofactor for fluorescence [7, 10]. Bilirubin is an open tetrapyrrole, and is the final breakdown product of heme metabolism [13]. Other tetrapyrrole ligands including biliverdin have recently been shown to be responsible for the red fluorescence in the walleye fish, *Sander vitreus*. Interestingly, the protein responsible for fluorescence is lipocalin, which along with fatty acid-binding proteins are part of the structural superfamily, calycin [14–16].

Here we present a study on a series of mutations in Chlopsid FP. One mutation is a deletion of a GPP (Gly-Pro-Pro) motif. The GPP motif is found throughout this class of fluorescent FABPs, but not in homologous non-fluorescent brain FABPs [6]. This motif was previously implicated in the fluorescence mechanism for Chlopsid FP. It was shown that when the two prolines were mutated to glycine, the fluorescent quantum yield was reduced from 0.47 (WT) to 0.11 [6]. Here we show deletion of this GPP motif results

Published online: 24 February 2020



[☐] Jean P. Gaffney jean.gaffney@baruch.cuny.edu

Department of Natural Sciences, Baruch College, City University of New York, New York, NY 10010, USA

The Graduate Center, Program in Biology, City University of New York, New York, NY 10016, USA

Department of Chemistry, Saint Peter's University, Jersey City, NJ 07306, USA

in a complete quenching of fluorescence, demonstrating the importance of this motif in the fluorescence mechanism.

In addition, we present a detailed study of point mutations of Chlopsid FP, focusing on residues that were implicated in bilirubin binding in UnaG [7–9]. We generated a panel of five mutants using site directed mutagenesis. We report quantum yields and binding constants of selected mutants.

Fatty acid-binding proteins (FABPs) are part of a larger family of intracellular lipid binding proteins (iLBPs), which are ubiquitous across species and tissues [17–19]. The primary function of FABPs is to not only transport fatty acids but also play a role in intracellular transport [17, 20]. This work will lead to the better understanding and characterization of these unique eel fluorescent fatty acid-binding proteins. Furthermore, UnaG has already been adapted for multiple assays including monitoring cellular redox state and measuring serum bilirubin levels [9, 21, 22]. Due to the high level of homology between UnaG and Chlospid FP, it is likely that Chlopsid FP is adaptable for cellular assays as well. Chlopsid FP also shows many advantages over GFP, due to its small molecular weight (16 KDa vs. 28 KDa) and compatibility with hypoxic conditions [10, 21, 23].

2 Materials and Methods

2.1 Reagents and Chemicals

All analytical grade chemicals and reagents were purchased from commercial sources. Isopropyl β -D-1-thiogalactopyranoside and bilirubin were purchased from Sigma-Aldrich. Additional reagents required to conduct assays included Fluorescein (Invitrogen), Lysozyme (AmericanBio), Kanamycin sulfate (Fisher scientific), Imidazole (EMD), and Coomassie Stain (InstantBlue). Pre-cast 12% polyacrylamide gels were purchased from Biorad.

2.2 Protein Expression and Purification

Mutant DNA sequences of Chlopsid FP were acquired from Genscript. These sequences contained the respective point mutations, as well as an IPTG-inducible promoter, a histidine tag, and a kanamycin resistance gene. The genes for WT and mutant Chlopsid FP were transformed in BL21(DE3) $E.\ coli$ cells (Millipore). Single colonies were selected and used to seed starter cultures in LB Media. Protein expression was induced using 0.1 mM IPTG when bacteria reached an OD₆₀₀ of 0.6.

Protein was purified using Ni-affinity chromatography, eluting with 50 mM Tris, 150 mM NaCl, and 300 mM imidazole, pH 8.0. The protein was dialyzed against 50 mM Tris HCl to remove imidazole and concentrated using an Amicon Ultra centrifugal concentrator (m.w.c.o. 3000).

Protein purity was confirmed using SDS-PAGE. Protein concentration was determined by A_{280} measurements with a Cary 60 UV–Vis, using the calculated extinction coefficient 15,768 M^{-1} cm⁻¹ for Chlopsid FP. Bilirubin (Sigma-Aldrich, USA) was dissolved in 0.1 M NaOH and immediately diluted in 50 mM Tris–HCl buffer, for use in experiments.

2.3 Preparation of Holo Chlopsid FP from Apo Chlopsid FP and Bilirubin

Bilirubin (Sigma-Aldrich) was dissolved in 0.1 M NaOH and then diluted with 50 mM Tris-HCl, pH 7.4. For preparation of holo Chlopsid FP, apo Chlopsid FP and bilirubin were mixed with 1:1 stoichiometry in 50 mM Tris HCl, pH 7.4. Formation of holo Chlopsid FP was confirmed using fluorescent spectroscopy.

2.4 Fluorescence Spectroscopy and Quantum Yield

Fluorescence excitation and emission spectra were recorded using a F-7000 Hitachi Fluorescence Spectrometer. Bilirubin and apo Chlopsid FP were combined in a 1:1 stoichiometry. For wild-type Chlopsid FP, fluorescence emission was measured at 523 nm following an excitation at 489 nm.

For all measurements, the solutions were measured at dilute concentrations to maintain the absorbance below 0.02. Fluorescein (Sigma) was used as a standard. Absorbance measurements of higher concentrations of fluorescein and the protein samples were made to confirm linearity before dilution was performed and the lower absorbance values were extrapolated. All absorbance measurements were made on a Cary 60 UV–Vis spectrophotometer.

For quantum yield calculations, the spectra were recorded and the software FL Solutions 4.0 was used to integrate the area under the emission peak. When the integrated fluorescence intensity was plotted against the absorbance, a linear relationship was seen. The linear curve was fit and the slope of the line was used to calculate the quantum yield as compared to fluorescein. Excel was used to perform the linear fit of the results. Quantum yield measurements were performed in triplicate.

2.5 Fluorescence Titrations

Fluorescence titrations were conducted by adding increasing concentrations of bilirubin to 500 nM Chlopsid FP (WT and mutants). Titrations were performed in triplicates and data from all three trials were averaged to create titration curves. The average titration of Chlopsid FP and the respective mutants were fitted using Kaleidagraph (Synergy Software) with a single-site binding model [24–26]



$$\frac{LR}{L} = ((R + L + Kd) - \sqrt{((R + L + Kd)^2 - 4 * R * L)})/(2 * L)$$

2.6 Structural Modeling

A three-dimensional (3-D) model of Chlopsid FP was predicted using Swiss Model (https://swissmodel.expasy.org/). The closest structure was UnaG, which was used as a template. UnaG's sequence is 58% homologous to Chlopsid FP [7]. The predicted structure was then rendered using PyMol [27].

3 Results

3.1 Using Comparative Modeling to Understand More About the Structure of ChlopsidFP

The structure of Chlopsid FP is expected to be similar to the crystal structure of UnaG, due to the high level of homology and similarity in function [7]. We used SWISS-MODEL to generate a predicted structure of Chlopsid FP (Fig. 1) [28–32]. Chlopsid FP shares 58% sequence homology with UnaG, allowing SWISS-MODEL to use the crystal structure of UnaG as a template for the predicted Chlopsid FP structure [6, 7]. PyMol was then used to render the structure generated by SWISS-MODEL. The GPP motif and other key residues mutated in the course of this study are highlighted (Fig. 1). The GPP motif, which distinguishes fluorescent FABPs from homologous, non-fluorescent FABPs, is shown on the exterior of the protein, on a loop adjacent to bilirubin [6]. Residues adjacent to the GPP motif, His56 and Pro60 are shown in pink and appear to interact with

the bilirubin inside of the β -barrel. Thr79, also shown in pink, sticks out into the interior of the β -barrel and appears to interact with bilirubin opposite of the His56 and Pro60 residues.

3.2 Chlopsid FP Binding of Bilirubin

For the wild-type Chlopsid FP we report a quantum yield of 0.47 and excitation/emission spectra of 489 nm and 523 nm respectively (Fig. 2). To assess the binding of bilirubin to Chlopsid FP and determine the dissociation constant titrations were run with a constant amount of protein (500 nM) with bilirubin being titrated (0–2 μ M). Data was fitted using a single-molecule binding model using Kaleidagraph software [24, 25]. We report a dissociation constant of 22.7 nM for wild type Chlopsid FP (Fig. 2).

When compared to the wild type Chlopsid FP at $10~\mu M$ concentrations, the GPP deletion mutant shows no quantifiable fluorescence (Fig. 2). Data was normalized to determine if fluorescence was absent or simply weakened, however the excitation and emission spectra observed with the wild type protein were not visible indicating fluorescence was quenched. To test if the GPP deletion mutant had a weaker affinity for bilirubin than the wild type a titration was performed, and no change was observed in the fluorescence (Fig. 2). The GPP deletion mutant showed no increase in fluorescence as the concentration of bilirubin increased.

3.3 Site-Directed Mutagenesis of Key Residues

Five point mutants were generated using site-directed mutagenesis to probe the residues implicated in fluorescence following bilirubin binding. Amino acids were chosen based

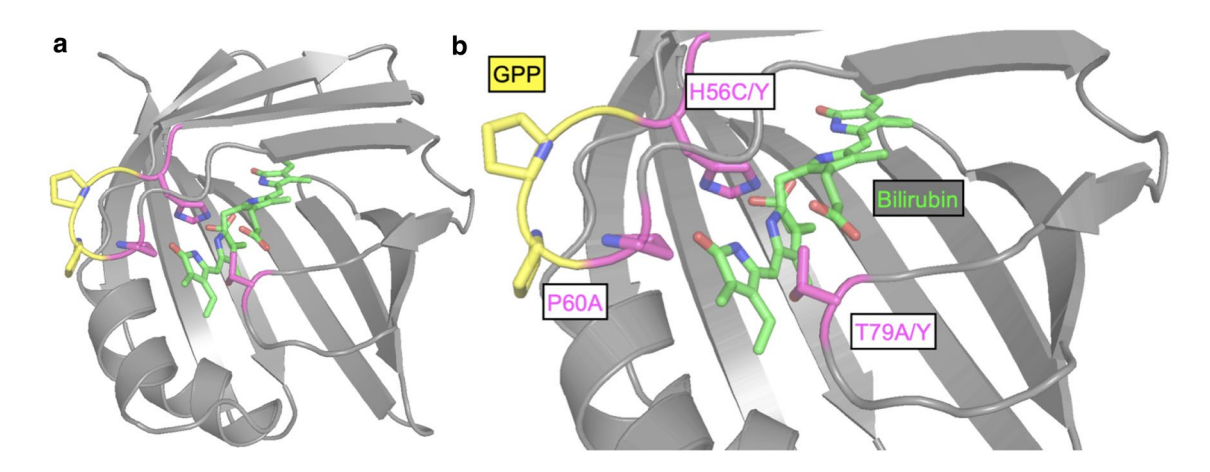
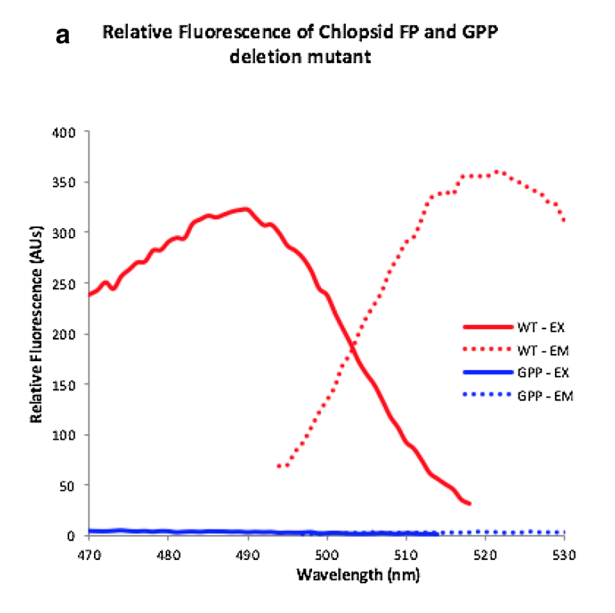
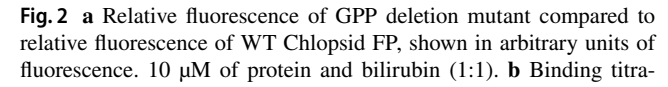


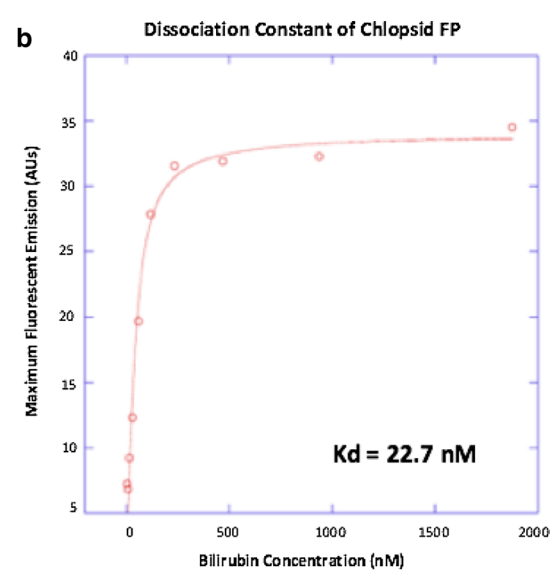
Fig. 1 a Proposed structure of Chlopsid FP using known homologous regions to UnaG (pdb 4I3B Ref. [7]). Fluorescence-inducing ligand, bilirubin, is shown in green in the center of the β -barrel. The yellow region depicts the GPP motif. Pink regions show the H56, P60, and

T79, residues, which were mutated using site directed mutagenesis. **b** Close-up of β -barrel and bilirubin binding residues (Color figure online)









tion of Chlopsid FP to bilirubin with Chlopsid FP concentration at 500 nM, fitted to a single-molecule binding model (Color figure online)

on prior findings regarding the crystal structure of UnaG and the model of Chlopsid FP (Fig. 1) [7, 9].

The wild type spectra of Chlopsid FP is blue shifted by 4 nm as compared to UnaG [6, 7]. For the wild type Chlopsid FP we report a quantum yield of 0.47 and excitation/emission spectra of 489 nm and 523 nm respectively (Fig. 2). Using a fluorescent intensity assay the dissociation constant of Chlopsid FP was calculated using a single-binding model. We report a dissociation constant of 22.7 nM (Fig. 2).

H56 in Chlopsid FP is an asparagine in UnaG [6]. This residue was implicated in bilirubin binding in UnaG and is located in close proximity to the GPP motif [7]. We mutated H56 to tyrosine and cysteine. Tyrosine was chosen to see if a large aromatic amino acid would cause a shift in the emission spectra. Cysteine was chosen to replace the histidine with a smaller amino acid. Alanine was not chosen since this work had been done with UnaG [7]. Equal concentrations of H56 mutants were then tested against wild type Chlopsid FP to examine changes in max excitation and max emission. Several trials showed that the His56 mutants either abolished or nearly abolished fluorescence with over a fourfold fluorescent decrease in H56C (Fig. 3a). Dissociation constant for H56C was measured at 24.7 nM (Fig. 3b). H56Y resulted in a significant decrease in fluorescence and a binding constant could not be measured.

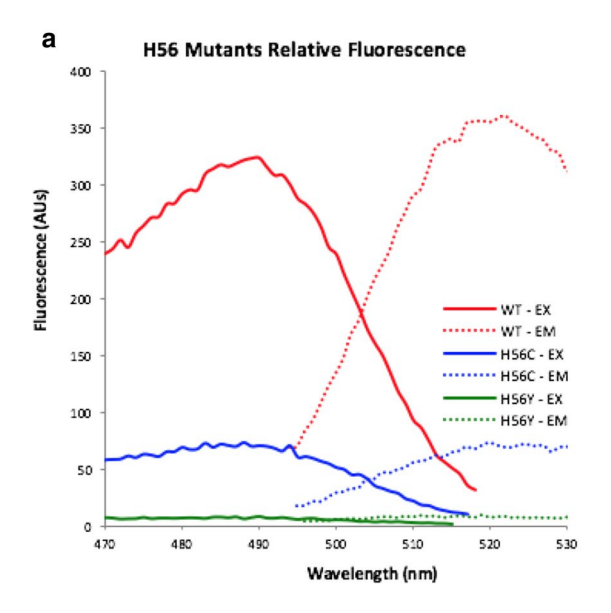
P60, a residue following the GPP insert in Chlopsid FP was chosen to probe the importance of the loop closure. P60 was mutated to alanine, removing the proline ring. With the P60A, we observed reduced fluorescence (Fig. 4).

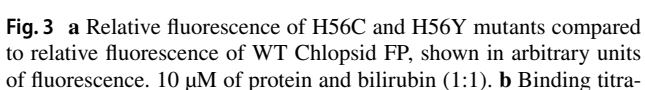
T79 was mutated to alanine, histidine and tyrosine. T79 was directly implicated in bilirubin binding in the structure of UnaG [7]. Mutation of T79 to alanine in Chlopsid FP resulted in a significant reduction in fluorescence (Fig. 5a). T79 to tyrosine also resulted in a significant decrease in fluorescence. No significant shift in the emission spectra was observed. T79A showed a threefold reduction in fluorescence intensity with a dissociation constant of 53.2 nM (Fig. 5). Furthermore, we report a reduced quantum yield of 0.22 in the T79A mutant. The binding constant of the T79Y mutant was not measurable due to a significant decrease in fluorescence intensity.

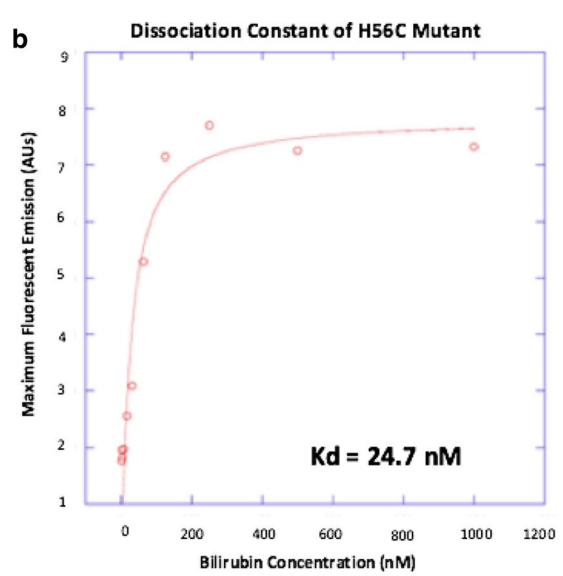
4 Discussion

Chlopsid FP is a novel fluorescent protein isolated from muscular tissue of the marine chlopsid eel, *K. hyoproroides* [6]. It displays a bright green fluorescence when excited with blue light (excitation and emission wavelengths are 489 nm and 523 nm respectively). Chlopsid FP joins a class of fluorescent fatty acid binding proteins from eels that require the addition of bilirubin for fluorescence. The first member of this class was identified in the aquaculture eel *Anguilla japonica*, and was later characterized and the crystal structure was solved [7, 10]. Fluorescent fatty acid binding proteins from eels are half the size of Green Fluorescent Protein, which may be useful for protein labeling applications [6, 7, 10, 11]. Furthermore, the fluorescent eel FABPs have









tion of H56C to bilirubin with His56C concentration at 500 nM, fitted to a single-molecule binding model (Color figure online)

P60 Mutants Relative Fluorescence

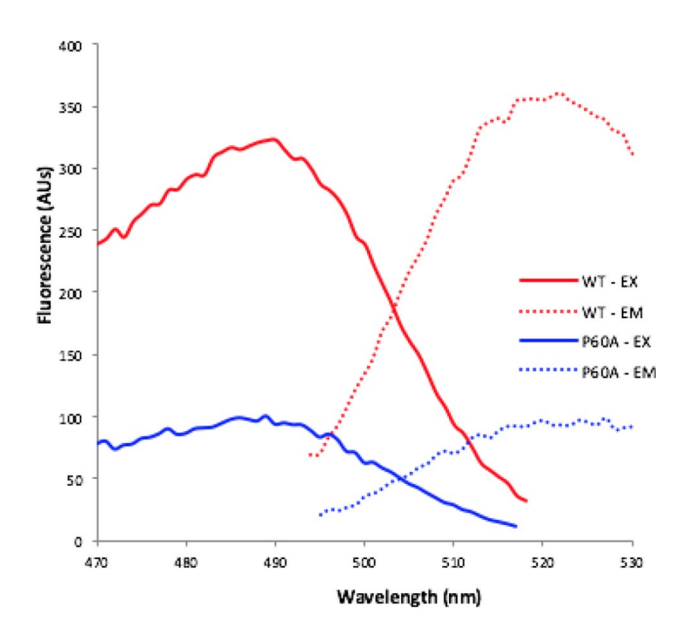


Fig. 4 Relative fluorescence of Pro60A mutant compared to relative fluorescence of WT Chlopsid FP, shown in arbitrary units of fluorescence. 10 μM of protein and bilirubin (1:1) (Color figure online)

been shown be stable in hypoxic conditions, allowing the potential to track proteins during autophagy [21].

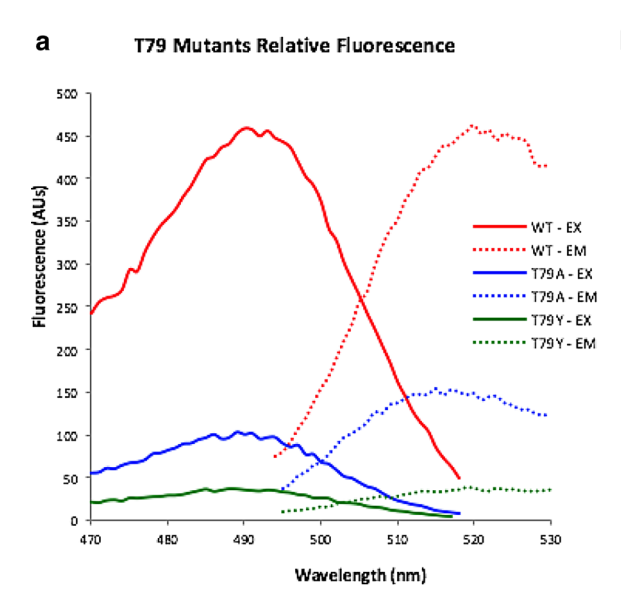
Our work aimed to understand more about the bilirubin binding residues in Chlopsid FP as well as a sequence insert implicated in fluorescence (GPP motif). The GPP motif is found in fluorescent FABPs, but not in homologous, non-fluorescent FABPs [6].

Our first goal was to determine the affinity of Chlopsid FP for bilirubin. Here we report a Kd of 22.7 nM for bilirubin binding to WT Chlopsid FP and show that when key residues around the GPP motif are mutated, not only does the fluorescent quantum yield decrease, but the affinity for bilirubin changes as well (Figs. 2, 3, 4).

To determine if the fluorescent spectra of Chlopsid FP could be shifted, we created a panel of five point mutations. As a result of our prior research, which identified a GPP motif, we focused on this region of the protein in creating our panel of point mutants. The mutants displayed significant changes in the fluorescent intensity as well as in binding bilirubin. The severe reduction in fluorescent intensity of these proteins supports the significance of the GPP motif as the H56 and P60 residues flank it. This supports our hypothesized structure of Chlopsid FP with a critical GPP loop. We hypothesize these mutations allowed more mobility in the loop and therefore the interior of the protein may be exposed to solvent.

After observing a reduced fluorescence intensity and quantum yield in several mutants we then looked at whether or not this was due to weaker binding of bilirubin or a change in the fluorophore formation. In general, we observed weaker binding in point mutants compared to wildtype Chlopsid FP. Of note, the H56C mutant showed low levels of fluorescence in comparison to wild type Chlopsid FP, however it had a dissociation constant of 24.7 nM. This dissociation constant is comparable to the 22.7 nM dissociation constant observed in Chlospid FP, indicating that this residue may play a role in fluorophore formation, not bilirubin binding.





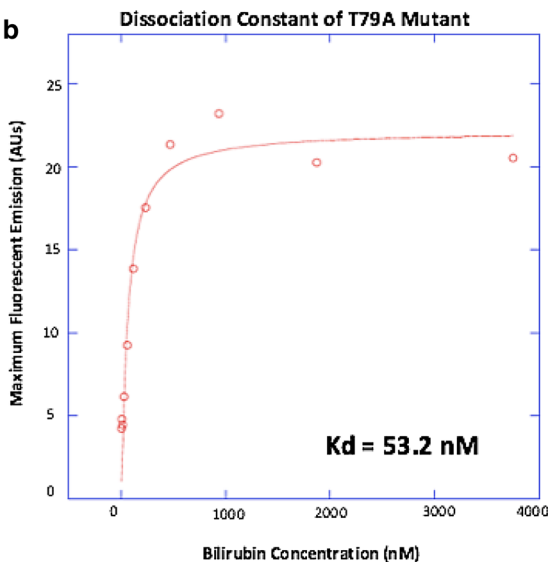


Fig. 5 a Relative fluorescence of T79A and T79Y mutants compared to relative fluorescence of WT Chlopsid FP, shown in arbitrary units of fluorescence. 10 μ M concentration of protein to bilirubin.

b Binding titration of T79A to bilirubin with T79A concentration at 500 nM, fitted to a single-molecule binding model (Color figure online)

To further examine the significance of the GPP motif we created a GPP deletion mutant. Several trials showed that no fluorescence was detected, even with increasing amounts of bilirubin. From this we conclude that deletion of the GPP motif abolishes the fluorophore, supporting it as the motif, which distinguishes fluorescent FABPs from non-fluorescent FABPs. Of note, further trials will need to be conducted to determine if the GPP deletion mutant binds bilirubin or if this too is abolished.

In conclusion, we have demonstrated key point mutations that lead to fluorescence quenching in Chlopsid FP. These mutations may provide further insight into the mechanism of fluorescence in eel fluorescent fatty acid binding proteins. We show that when key residues near an integral GPP motif are mutated the intensity of fluorescence is severely reduced or lost. This reduced fluorescence corresponds with a reduced affinity for bilirubin in most of the mutants, with the exception of a H56C adjacent to the GPP motif. The strong affinity of the H56C mutant for bilirubin, suggests that this part of the protein plays a role in the formation of the fluorophore not in binding bilirubin. Thus, providing further evidence that the GPP motif is responsible for formation of the fluorophore of the protein. Complete abolishment of fluorescence when the GPP motif is deleted further supports this role.

Moving forward a continued understanding of the Chlopsid FP will help to better adapt the protein for biotechnological assays. Already the homologous UnaG protein has been used in multiple biomedical assays including measurement of serum bilirubin levels and examining hypoxic conditions

[9, 21, 22, 33]. The next step to understanding the structure and binding of Chlopsid FP is to solve the crystalline structure of not only the holo protein, but also the apo protein, something, which has yet to be done for any member of the homologous bilirubin-induced fluorescent FABP family.

Acknowledgements This work was supported by a National Science Foundation Career Grant to J.P.G (Award Number MCB 1652731). We would like to thank Professor Pablo Peixoto for use of his fluorimeter.

Compliance with Ethical Standards

Conflict of interest The authors declare no conflict of interest.

References

- Sparks JS, Schelly RC, Smith WL et al (2014) The covert world of fish biofluorescence: a phylogenetically widespread and phenotypically variable phenomenon. PLoS ONE 9:e83259. https:// doi.org/10.1371/journal.pone.0083259
- Gruber DF, Loew ER, Deheyn DD et al (2016) Biofluorescence in catsharks (Scyliorhinidae): fundamental description and relevance for elasmobranch visual ecology. Sci Rep. https://doi.org/10.1038/ srep24751
- Salih A, Larkum A, Cox G et al (2000) Fluorescent pigments in corals are photoprotective. Nature 408:850. https://doi. org/10.1038/35048564
- Rye C, Wise R, Jurukovski V, et al Aquatic biomes: biology 2e. OpenStax
- Tyler J (1968) JERLOV, N. G. 1968. Optical oceanography. American Elsevier Publ. Co., Inc, New York. 194 p. \$13.50. Limnol Oceanogr 13:731–732. https://doi.org/10.4319/lo.1968.13.4.0731



- Gruber DF, Gaffney JP, Mehr S et al (2015) Adaptive evolution of eel fluorescent proteins from fatty acid binding proteins produces bright fluorescence in the marine environment. PLoS ONE. https://doi.org/10.1371/journal.pone.0140972
- Kumagai A, Ando R, Miyatake H et al (2013) A bilirubin-inducible fluorescent protein from eel muscle. Cell 153:1602–1611. https://doi.org/10.1016/j.cell.2013.05.038
- Shitashima Y, Shimozawa T, Kumagai A et al (2017) Two distinct fluorescence states of the ligand-induced green fluorescent protein UnaG. Biophys J 113:2805–2814. https://doi.org/10.1016/j. bpj.2017.10.022
- Shitashima Y, Shimozawa T, Asahi T, Miyawaki A (2018) A dual-ligand-modulable fluorescent protein based on UnaG and calmodulin. Biochem Biophys Res Commun 496:872–879. https://doi.org/10.1016/j.bbrc.2018.01.134
- Hayashi S, Toda Y (2009) A novel fluorescent protein purified from eel muscle. Fish Sci 75:1461–1469. https://doi.org/10.1007/ s12562-009-0176-z
- Funahashi A, Itakura T, Hassanin AAI et al (2017) Ubiquitous distribution of fluorescent protein in muscles of four species and two subspecies of eel (genus Anguilla). J Genet 96:127–133. https://doi.org/10.1007/s12041-017-0751-5
- Aoyama J, Nishida M, Tsukamoto K (2001) Molecular phylogeny and evolution of the freshwater eel, genus anguilla. Mol Phylogenet Evol 20:450–459. https://doi.org/10.1006/mpev.2001.0959
- Broichhagen J, Trauner D (2013) Bilirubin in a new light. Angew Chem Int Ed 52:13868–13870. https://doi.org/10.1002/anie.20130 7345
- Yu C-L, Ferraro D, Ramaswamy S et al (2008) Purification and properties of Sandercyanin, a blue protein secreted in the mucus of blue forms of walleye, *Sander vitreus*. Environ Biol Fish 82:51– 58. https://doi.org/10.1007/s10641-007-9252-3
- Ghosh S, Yu C-L, Ferraro DJ et al (2016) Blue protein with red fluorescence. PNAS 113:11513–11518. https://doi.org/10.1073/ pnas.1525622113
- Flower DR (1996) The lipocalin protein family: structure and function. Biochem J 318:1–14
- Storch J, Thumser AEA (2000) The fatty acid transport function of fatty acid-binding proteins. Biochem Biophys Acta 1486:28–44. https://doi.org/10.1016/S1388-1981(00)00046-9
- Zimmerman AW, Veerkamp JH (2002) New insights into the structure and function of fatty acid-binding proteins. Cell Mol Life Sci 59:1096–1116. https://doi.org/10.1007/s00018-002-8490-y
- Schaap FG, van der Vusse GJ, Glatz JFC (2002) Evolution of the family of intracellular lipid binding proteins in vertebrates. In: Glatz JFC (ed) Cellular lipid binding proteins. Springer, Boston, pp 69–77
- Chmurzyńska A (2006) The multigene family of fatty acid-binding proteins (FABPs): function, structure and polymorphism. J Appl Genet 47:39–48. https://doi.org/10.1007/BF03194597

- Hu H, Wang A, Huang L et al (2018) Monitoring cellular redox state under hypoxia using a fluorescent sensor based on eel fluorescent protein. Free Radical Biol Med 120:255–265. https://doi. org/10.1016/j.freeradbiomed.2018.03.041
- Adeosun SO, Moore KH, Lang DM, et al. (2018) A novel fluorescence-based assay for the measurement of biliverdin reductase activity. React Oxyg Species 5:35–45. https://doi.org/10.20455/ros.2018.809
- Inoué S, Shimomura O, Goda M et al (2002) Fluorescence polarization of green fluorescence protein. Proc Natl Acad Sci USA 99:4272–4277. https://doi.org/10.1073/pnas.062065199
- Pollard TD (2010) A guide to simple and informative binding assays. Mol Biol Cell 21:4061–4067. https://doi.org/10.1091/mbc. E10-08-0683
- 25. KaleidaGraph. Synergy Software
- Hulme EC, Trevethick MA (2010) Ligand binding assays at equilibrium: validation and interpretation. Br J Pharmacol 161:1219–1237. https://doi.org/10.1111/j.1476-5381.2009.00604
- The PyMOL Molecular Graphics System. Version 2.0. Schrodinger, LLC
- Waterhouse A, Bertoni M, Bienert S et al (2018) SWISS-MODEL: homology modelling of protein structures and complexes. Nucleic Acids Res 46:W296–W303. https://doi.org/10.1093/nar/gky427
- Bienert S, Waterhouse A, de Beer TAP et al (2017) The SWISS-MODEL repository-new features and functionality. Nucleic Acids Res 45:D313–D319. https://doi.org/10.1093/nar/gkw1132
- Guex N, Peitsch MC, Schwede T (2009) Automated comparative protein structure modeling with SWISS-MODEL and Swiss-PdbViewer: a historical perspective. Electrophoresis 30(Suppl 1):S162–173. https://doi.org/10.1002/elps.200900140
- Benkert P, Biasini M, Schwede T (2011) Toward the estimation of the absolute quality of individual protein structure models. Bioinformatics 27:343–350. https://doi.org/10.1093/bioinformatics/ btq662
- Bertoni M, Kiefer F, Biasini M et al (2017) Modeling protein quaternary structure of homo- and hetero-oligomers beyond binary interactions by homology. Sci Rep. https://doi.org/10.1038/s41598-017-09654-8
- Yeh JT-H, Nam K, Yeh JT-H, Perrimon N (2017) eUnaG: a new ligand-inducible fluorescent reporter to detect drug transporter activity in live cells. Sci Rep. https://doi.org/10.1038/srep41619

Publisher's Note Springer Nature remains neutral with regard to jurisdictional claims in published maps and institutional affiliations.

